FEBS Letters 583 (2009) 1349–1357

FEBS Letters

journal homepage: www.FEBSLetters.org

The C-terminal cytoplasmic domain of human proEGF is a negative modulator of body and organ weights in transgenic mice

Thomas Klonisch [a,b,*,1], Aleksandra Glogowska [a,1], Ana A. Gratao [c], Marjeta Grzech [c], Andreea Nistor [a], Mark Torchia [d], Ekkehard Weber [e], Martin Hrabé de Angelis [f], Birgit Rathkolb [c,g], Cuong Hoang-Vu [h], Eckhard Wolf [c], Marlon R. Schneider [c]

[a] Department of Human Anatomy and Cell Science, University of Manitoba, 130-745 Bannatyne Avenue, Winnipeg, Canada R3E0J9
[b] Department of Medical Microbiology and Infectious Diseases, University of Manitoba, 130-745 Bannatyne Avenue, Winnipeg, Canada R3E0J9
[c] Chair for Molecular Animal Breeding and Biotechnology, and Laboratory for Functional Genome Analysis (LAFUGA), Gene Center, LMU Munich, Munich, Germany
[d] Department of Surgery, University of Manitoba, GF547-820 Sherbrook Street, Winnipeg, Canada R3A 1R9
[e] Institute of Physiological Chemistry, Martin Luther University of Halle-Wittenberg, Halle/Saale, Germany
[f] Institute of Experimental Genetics, Helmholtz Center Munich, Oberschleissheim, Germany
[g] German Mouse Clinic, Helmholtz Center Munich, Oberschleissheim, Germany
[h] Clinics of Surgery, Martin Luther University of Halle-Wittenberg, Halle/Saale, Germany

ARTICLE INFO

Article history:
Received 7 February 2009
Revised 17 March 2009
Accepted 21 March 2009
Available online 27 March 2009

Edited by Laszlo Nagy

Keywords:
proEGF cytoplasmic domain
Kidney
Transgenic
Growth
IGFBP-3

ABSTRACT

We generated transgenic mice to study the in vivo role of the cytoplasmic domain of human proEGF (proEGFcyt). Post-pubertal proEGFcyt transgenic (tg) mice displayed an up to 15% reduction in body weight, including smaller kidney and brain weights as compared to control littermates. Renal histology, gene expression profiles, and functional parameters were normal. In both sexes, serum levels of IGFBP-3 were reduced. Circulating IGF-I/IGF-II levels were unchanged. Histomorphological analysis revealed isolated foci of liver necrosis specific to proEGFcyt tg mice. In conclusion, we identified proEGF cytoplasmic domain as a novel modulator of whole body and organ-specific growth in mice.

1. Introduction

The membrane-anchored proform of the largest epidermal growth factor (EGF)-like precursor, proEGF, contains the largest cytoplasmic domain (155 aa; proEGFcyt) of all EGFR ligands [1]. Cytoplasmic domains of proEGF-like ligands are biologically active and have multiple cellular functions [2–8]. Transgenic (tg) mice expressing human full-length proEGF under the control of a beta-actin promoter showed stunted growth, abnormalities of osteoblasts, focal liver necrosis, and infertility [9,10]. This complex phenotype was distinct from that of transforming growth factor-alpha (TGFA) tg mice [11,12], but showed similarities with the phenotypes of tg mice overexpressing heparin-binding EGF-like growth factor (HBEGF) [13] or betacellulin [14]. We generated tg mice overexpressing human proEGFcyt under the control of a chicken beta-actin promoter and found that proEGFcyt contributed to some but not all reported phenotypical changes observed with the full-size proEGF tg mice [9,10].

2. Materials and methods

2.1. RNA-processing, RT-PCR, Northern blot

Total RNA isolation, first strand cDNA synthesis, and semiquantitative RT-PCR were performed as described earlier [2,3]. Primers and PCR conditions were used as described previously [15]. Northern blot analysis was done as described previously [14] using random prime-labeled cDNA probes.

2.2. Transgene construction and generation of transgenic mice

An *Eco*RI fragment of human proEGFcyt [3] was cloned downstream of the cytomegalovirus enhancer, chicken β-actin

* Corresponding author. Address: Department of Human Anatomy and Cell Science, University of Manitoba, 130-745 Bannatyne Avenue, Winnipeg, Canada R3E0J9.
E-mail address: klonisch@cc.umanitoba.ca (T. Klonisch).
[1] Both authors contributed equally to this work.

0014-5793/$36.00
doi:10.1016/j.febslet.2009.03.051

promoter and rabbit β-globin splice acceptor, and upstream to the rabbit β-globin 3′-flanking region and polyadenylation signal in the expression vector pUC-CAGGS (Fig. 1A). Transgenic mice were generated by pronuclear injection of the constructs (diluted to 1–2 ng/μl) into fertilized FVB/N oocytes [14]. Founders were identified by PCR and mated to wild-type FVB/N animals. All animal experiments were approved by the institutional animal care committee and carried out in accordance with the German Animal Protection Law.

2.3. Growth analyses, pathology, clinical chemistry

Litters were weighed weekly from 3 to 12 weeks of age. Animals were bled under ether anesthesia and then sacrificed. Organs were dissected, blotted dry, and weighed to the nearest mg. Tissue samples were taken and frozen at −80 °C or fixed in Bouin's solution (Sigma), processed, and embedded in paraffin for histological examination and staining with hematoxylin/eosin (H&E). Mouse serum samples were diluted 1:2 with deionised water (except for magnesium measurement, which was done on undiluted samples) and centrifuged for 10 min at 4700×*g* to remove clots. An Olympus AU 400 autoanalyzer was used to determine electrolyte, total protein, creatinine levels, and serum activities for α-amylase, alanine aminotransferase, aspartate aminotransferase, alkaline phosphatase, creatine kinase, and lipase.

2.4. Detection of cleaved proEGFcyt in stable MCF-7 transfectants

The production of the rabbit (rb) antiserum against human proEGFcyt has been described previously [2]. The anti-proEGFcyt and anti-FLAG M2 antisera (Sigma) were used in Western blots (both 1:1000) and immunoprecipitation (both 1:100) on stable transfectants of the human breast cancer cell line MCF-7 expressing Xpress-tagged human proEGFcyt, membrane-anchored proEGF with C-terminal FLAG tag (proEGFctF; generously provided by Dr. H.S. Wiley), and empty vector, respectively [2,3]. For binding inhibition assays, GST-proEGFcyt (8 μg/ml) was pre-incubated for 2 h at 4 °C with the proEGFyt antiserum prior to Western blot. Detection of human proEGFcyt in mouse tissue extracts (20 μg/ml) was done with the proEGFcyt antiserum (1:1000).

2.4. Immunohistochemistry

Non-specific binding was blocked with 3% BSA and 10% goat normal serum or 10% rb normal serum (for the detection of mouse EGF) (both Sigma). Tissue sections (5 μm) were incubated overnight at 4 °C with proEGFcyt antiserum at 1:100, goat anti-mouse EGF (1:200; R&D Systems, MN, USA), rabbit anti-aquaporin-1 and anti-calbindin-D (K28) (both 1:250; Calbiochem, NJ, USA). Sections were incubated with the appropriate secondary antibodies (1:300; New England Bio Labs) and developed using DAB kit.

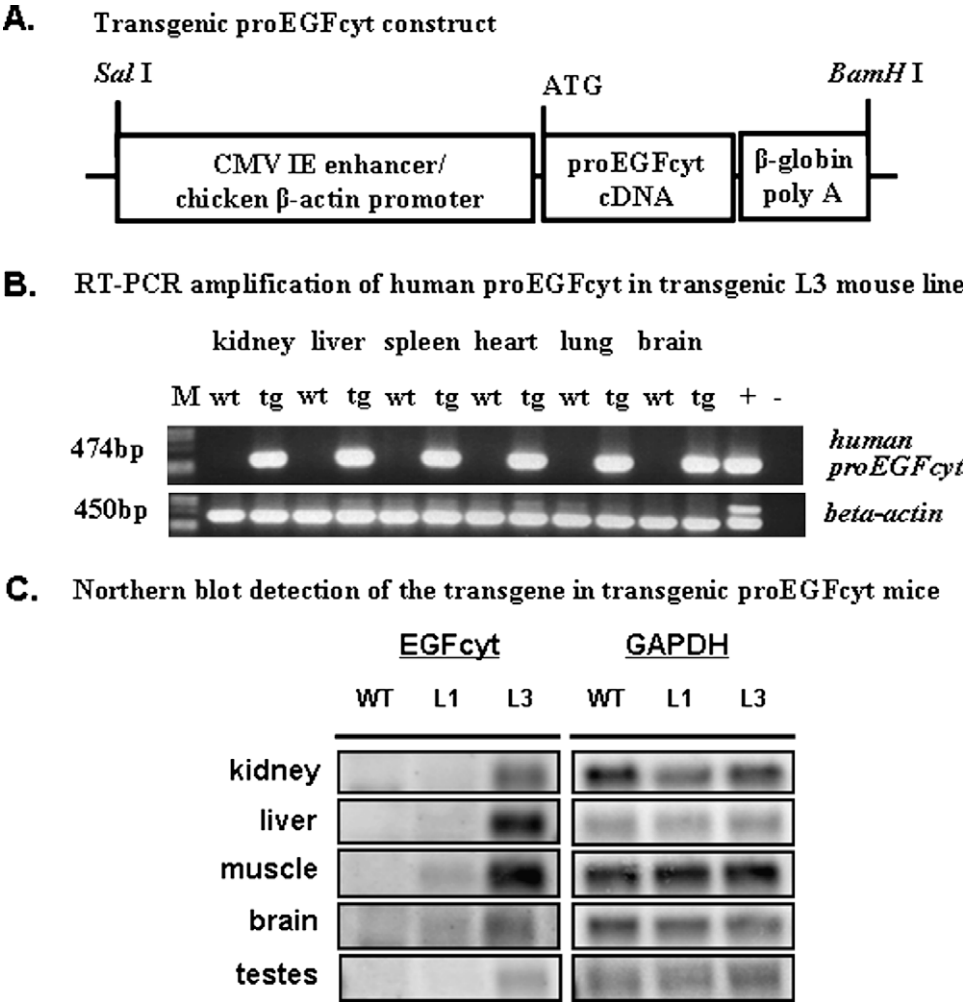

Fig. 1. (A) Schematic of the construct used in generating proEGFcyt tg mice. (B) RT-PCR analysis of transgene expression in various tissues of tg mice (L3); same results were obtained for L1. (C) Northern blot detection of transcripts encoding human proEGFcyt in mouse tissues of female L1 and L3 tg and normal littermates.

2.5. Measurement of IGFs and IGFBPs in serum

Determination of serum IGF-I, IGF-II, and IGFBP-1 to -5 levels were quantified as described previously [16–18].

2.6. Statistics

All experiments were repeated at least three times. For growth and weight measurements, the mean values with standard errors are shown and independent two-tailed *t*-test was performed, with $P < 0.05$ considered significant. For multiple group comparison, ANOVA table and Tukey's test were used with $P < 0.05$ being regarded significant.

3. Results

Two tg mouse lines (L1 and L3) expressing human proEGFcyt (Fig. 1A) were established and transmitted the transgene in a mendelian fashion. Transcripts for human proEGFcyt were detected by RT-PCR (L3; Fig. 1B) and Northern blot analysis (Fig. 1C). A specific antiserum against human proEGFcyt immunoprecipitated human Xpress-tagged proEGFcyt protein from extracts of MCF-7-proEGFcyt transfectants expressing soluble human proEGFcyt (Fig 2A). Specific binding of this antiserum to proEGFcyt was blocked by pre-incubation with GST-proEGFcyt protein (Fig. 2B). The proEGFcyt antiserum failed to detect mouse proEGF in mouse tissue extracts but specifically detected immunoreactive human proEGFcyt in transgenic mouse tissues (Fig. 2C). To determine if proEGFcyt can be detected as a naturally cleaved product, we generated stable MCF-7-proEGFctF transfectants which express a previously described membrane-anchored construct of human proEGF with C-terminally FLAG-tagged cytoplasmic domain [19,20]. Using both antisera against FLAG (M2) and proEGFcyt, immunoprecipitates of MCF-7-proEGFctF revealed a band of immunoreactive membrane-bound proEGF (Fig. 3A). In addition, we detected a second band of lower molecular weight corresponding to cleaved proEGF cytoplasmic domain as determined by Western blot analysis of immunoprecipitates from MCF-7-proEGFcyt

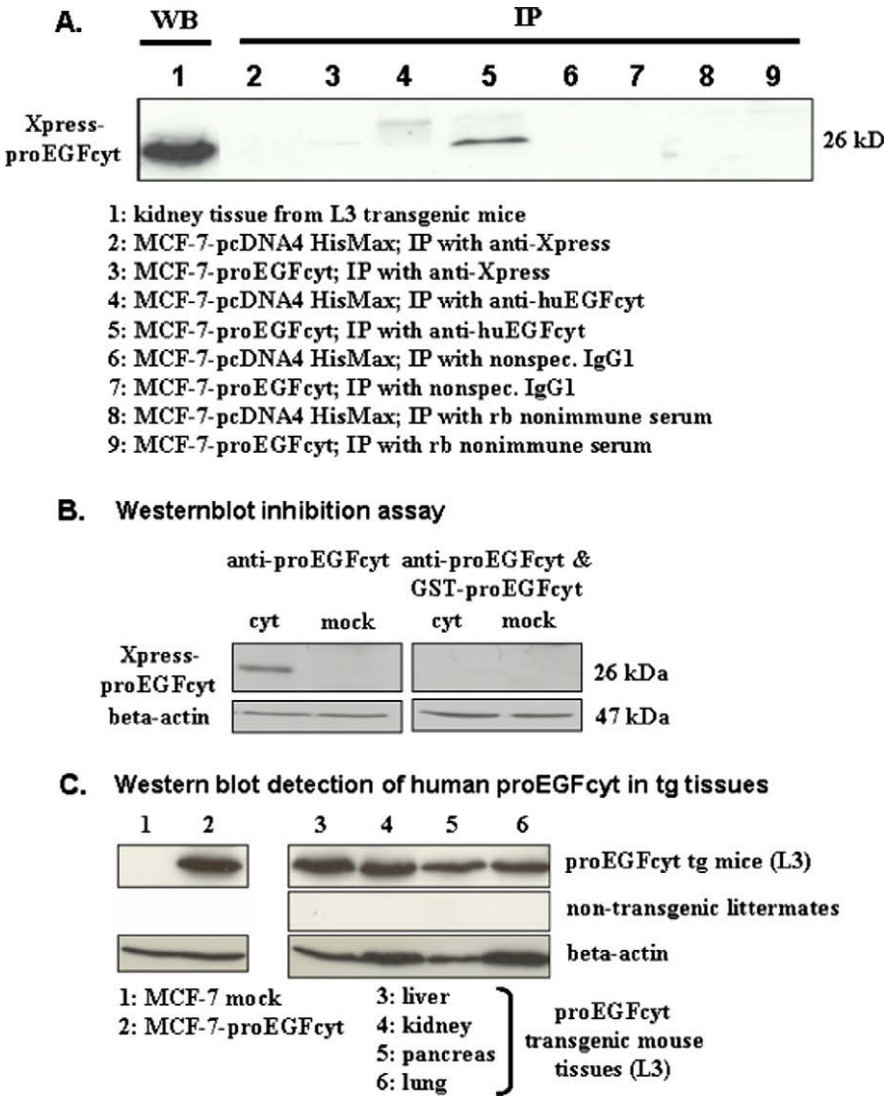

Fig. 2. (A) A rabbit (rb) anti-human proEGFcyt immunoprecipitated Xpress-tagged human proEGFcyt from MCF-7-proEGFcyt stable transfectants. Protein extracts of this transfectant served as positive control (lane 1). ProEGFcyt protein was exclusively detected when proEGFcyt antiserum was employed on MCF-7-proEGFcyt transfectants (lane 5). (B) Preincubation of the rb anti-human proEGFcyt with GST-proEGFcyt abolished detection of the Xpress-proEGFcyt fusion protein by either anti-Xpress or anti-proEGFcyt antiserum in Western blots of extracts from MCF-7-proEGFcyt transfectants. (C) Rb anti-proEGFcyt detected human proEGFcyt in tissue extracts of proEGFcyt tg mice but not in tissues of normal littermates (lanes 3–6). MCF-7-mock and MCF-7-proEGFcyt stable transfectants served as negative and positive control, respectively.

with the antiserum against proEGFcyt (Fig. 3A). Immunodetection of both proteins by the antiserum against proEGFcyt was blocked completely by pre-incubation with recombinant GST-proEGFcyt (Fig. 3B). Thus, in MCF-7-proEGFctF transfectants the membrane-anchored proEGFctF was cleaved to release a soluble cytoplasmic proEGF domain (Fig. 3A and B) validating our transgenic approach and indicating that the presence of soluble proEGFcyt cleaved product occurs naturally.

ProEGFcyt tg mice (L3) developed post-pubertal growth reduction of 15% (females) and 10% (males) compared to non-transgenic littermates as monitored during 3–12 weeks of postnatal life (Fig. 4A). Growth reduction remained constant at 5 months of age (Fig. 4B) when organ weights were evaluated (Table 1). L1 tg proEGFcyt animals with low levels of transgene expression were similar to control littermates. Thus, a specific threshold level of proEGFcyt was required to induce growth retardation. Tg mice from both genders consistently displayed a significant reduction in absolute weight of the brain (male ca. 10%; female ca. 15%) and kidney (ca. 20% for both sexes) as determined at 5 months of age (Table 1 and Fig. 5A). The reduced kidney weight was evident at 2 months of age (Fig. 5B), remained constant in females, and decreased further with age in male tg mice (Fig. 5B). Renal p38 MAPK phosphorylation [18] and p42/44 ERK have been implicated in renal development [21] but we failed to detect differences in the phosphorylation status of p38 or p42/44 in renal tissues of proEGFcyt tg mice (data not shown).

Kidney histology from proEGFcyt tg mice and wild-type littermates was normal. Immunoreactive human proEGFcyt was detected in aquaporin-(AQ-)1-immunopositive tubular cells (Fig. 6I) of the thick ascending loop of Henle (TAL; Fig. 6A, C, and E) of the outer and inner medullar region and in cells of the distal convoluted tubule (CT; Fig. 6G). The proximal nephron, including glomerulus, proximal tubule, and calbindin-D (K28)-immunopositive cells of the thin descending loop of Henle (Fig. 6K), were devoid of proEGFcyt. Instead, human proEGFcyt was localized to the basal tubular epithelial cell compartment (Fig. 6G) while mouse proEGF was immunolocalized to the apical membrane (Fig. 6M). Kidney sections from control mice were devoid of proEGFcyt immunoreactivity (data not shown). proEGFcyt tg mice are fertile and display normal bone structure (data not shown), but showed isolated foci of liver necrosis (Fig. 6O) not observed in control mice.

Reduced kidney weight in male and female proEGFcyt tg mice was not associated with altered renal expression patterns or decreased kidney function. We failed to detect differences in gene expression of key renal factors, including NKA, NKCC2, NHE3, CIC-K2, ROMK, ENaC, Barttin, renin, and Tamm Horsfall in kidneys of proEGFcyt and controls; NCC and COX2 were undetectable [15]. Serum levels of Na^+ and Cl^- (Fig. 7A), K^+, Mg^{2+}, Ca^{2+}, inorganic phos-

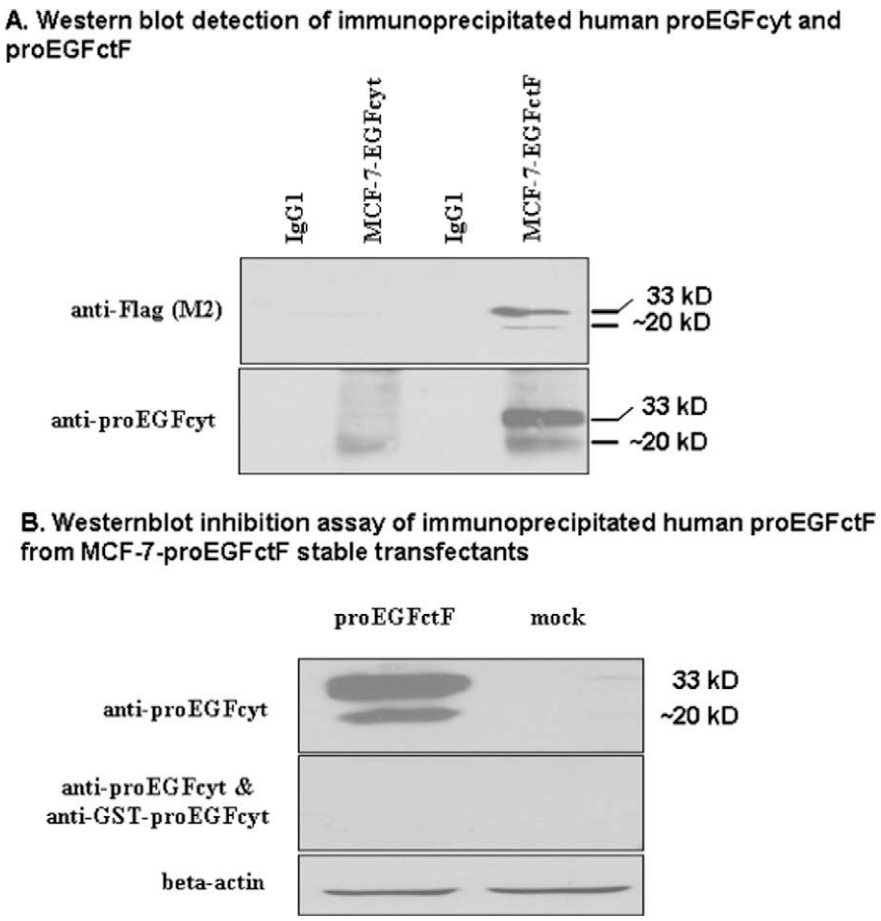

Fig. 3. (A) Rabbit anti-human proEGFcyt and FLAG antisera were employed to immunoprecipitate and detect in Western blots Xpress-tagged human proEGFcyt from MCF-7-proEGFcyt stable transfectants and human C-terminally FLAG-tagged proEGFctF from MCF-7-proEGFctF stable transfectants. The latter showed two distinct bands resembling membrane-anchored proEGFctF and a truncated FLAG-tagged protein of ca. 20 kDa, similar in size to soluble proEGFcyt which was immunoprecipitated with the rb anti-human proEGFcyt antiserum from MCF-7-proEGFcyt transfectants. (B) Preincubation of the rb anti-human proEGFcyt with GST-proEGFcyt abolished detection of both proEGFctF and the 20 kDa truncated protein by anti-proEGFcyt antiserum in Western blots of extracts from stable MCF-7-proEGFctF transfectants. Thus, the two immunoprecipitated FLAG-tagged proteins both contained proEGFcyt. This provided first evidence for a physiological presence of soluble proEGFcyt as a result of naturally occurring cleavage from the membrane-bound EGF proform in human cells and validated the transgenic approach described here. IgG1 isotype antisera served as negative controls for the immunoprecipitation.

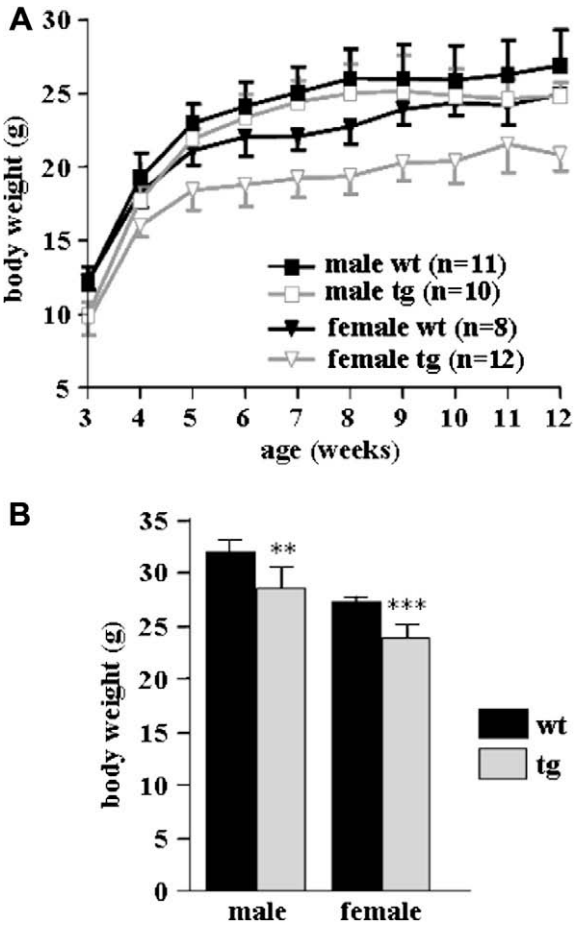

Fig. 4. (A) Weekly body weight measurements (3–12 weeks) revealed a significant reduction in postnatal body weight in L3 proEGFcyt tg animals compared to sex-/age-matched littermates. The differences in body weights were more pronounced in post-pubertal females than in male mice. The number of animals used is indicated in the graph and data are expressed as means ± S.E.M. (B) At the age of 5 months, L3 proEGFcyt tg mice displayed up to 15% reduction in body weight ($n = 8$ animals/group; data are shown as means ± S.E.M.).

phorus, creatinine, and total protein (Fig. 7B) were normal. Thus, reduced kidney weight in proEGFcyt tg mice did not coincide with altered gene expression pattern or reduced kidney functions.

Insulin-like growth factors (IGFs) and IGF-binding proteins (IGFBPs) are important in the control of body/organ growth [18,22–24]. We did not observe differences in serum IGF-I and IGF-II levels between transgenic and non-transgenic littermates (Fig. 8A). Western ligand blots revealed similar serum levels of IGFBP-1, -2, -4, and -5, but a marked down-regulation of IGFBP-3 in proEGFcyt tg mice compared to non-transgenic littermates (Fig. 8B).

4. Discussion

Here we report the generation of transgenic mice expressing human proEGFcyt and demonstrate for the first time an in vivo role of human proEGFcyt as a negative modulator of body mass and specific organ weights (kidney and brain). We also provide unique evidence from our MCF-7 human breast cancer cell model for a physiological cleavage of free cytoplasmic domain from membrane-anchored proEGF. This extends the list of EGFR ligands showing that the cytoplasmic domain is proteolytically cleaved from the membrane-bound proform. We had shown previously that human proEGFcyt is a modulator of microtubule dynamics and microtubule-associated protein (MAP) 1 and MAP2 production in human thyroid carcinoma [3]. Free cytoplasmic domains from other EGF-like ligands were shown to elicit important functional roles in the maturation, basolateral sorting, and intracellular trafficking of membrane proteins [4,25–30]. EGFR ligand cytoplasmic domains may also be clinically relevant by affecting cell proliferation and survival, as demonstrated for proHBEGFcyt [5–7,31].

Transgenic mice expressing the full-length human proEGF displayed 22% growth retardation at adulthood [9]. The proEGFcyt tg mice showed a similar albeit milder growth retardation of up to 15% in body weight in post-pubertal animals. As with full-size proEGF tg mice, proEGFcyt tg mice showed isolated foci of liver necrosis but failed to display abnormal ossification and infertility [9,10]. The proEGFcyt tg phenotype reflected distinct domain-specific in vivo functions of proEGFcyt which did not require the presence of full-size proEGF. One of those functions was the reduction in serum IGFBP-3 levels observed in both proEGF and proEGFcyt tg mice [9] which coincided with a growth retardation in both tg models. Serum levels of IGFBP-3 are known to be positively associated with body and organ mass [32] and inversely related to serum levels of IGF-I [33]. Rats treated with soluble EGF displayed decreased levels of circulating IGF-I as a result of a reduction in serum IGFBP-3 which is required for the binding of the majority of IGF-I in the serum as a ternary complex between IGFBP-3, IGF-I, and the acid-labile subunit (ALS) [24,34]. Stunted growth of tg mice expressing human proEGF was hypothesized to be a direct effect of extracellular EGF decreasing the secretion of IGFBP-3 [9].

Table 1
Absolute organ weights (mg) of female and male non-transgenic (wt) and EGFcyt tg mice from L1 and L3 at the age of 5 months. The table shows calculated mean values (±S.E.M.). A *t*-test was used to show absence (–) or presence ($^{*}P < 0.05$; $^{**}P < 0.01$; $^{***}P < 0.001$) of a statistically significant difference (Δ) between groups.

Organs	Organ weight (mg)									
	Females					Males				
	WT	Tg (L1)	Δ	Tg (L3)	Δ	WT	Tg (L1)	Δ	Tg (L3)	Δ
Kidneys	337 (15)	329 (21)	–	279 (23)	***	531 (35)	493 (15)	*	430 (30)	***
Brain	513 (20)	499 (6.2)	–	453 (8.7)	***	489 (18)	465 (18.7)	*	454 (11)	**
Lungs	160 (3.9)	169 (11)	–	145 (10)	**	169 (9.2)	163 (9.8)	–	164 (13)	–
Heart	128 (7.6)	114 (9.5)	*	117 (7.0)	*	143 (12)	124 (11)	*	144 (22)	–
Liver	1414 (130)	1503 (87)	–	1412 (105)	–	1607 (86)	1540 (150)	–	1598 (212)	–
Pancreas	289 (20)	281 (22)	–	271 (43)	–	283 (19)	264 (18)	–	274 (30)	–
Spleen	138 (15)	137 (19)	–	159 (32)	–	106 (4.5)	100 (11)	–	127 (35)	–
Adrenal glands	11.2 (1.6)	9.8 (1.2)	–	10.3 (1.9)	–	3.6 (1.5)	3.1 (0.7)	–	4.3 (1.6)	–
Uterus	85.5 (26)	68.0 (16)	–	80.4 (24)	–					
Ovaries	12.2 (6.3)	17.7 (2.1)	–	11.9 (4.7)	–					
Testis						195 (21)	189 (7.4)	–	196 (12)	–
Carcass (g)	9.92 (0.3)	10.23 (0.55)	–	8.30 (0.4)	***	11.13 (0.50)	10.4 (0.73)	–	10.6 (0.95)	–
n	6	6		8		7	6		6	

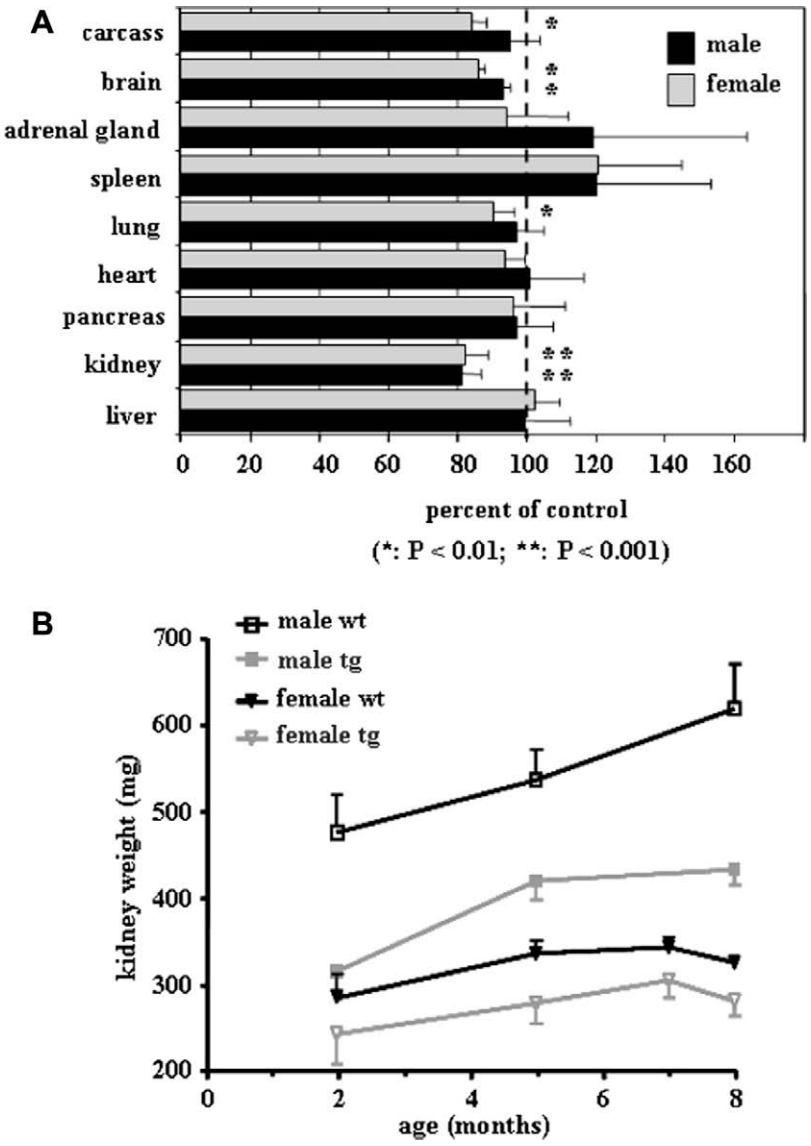

Fig. 5. (A) Absolute body and organ weights of proEGFcyt tg mice. Kidney and brain showed a significant and gender-independent decrease in weight compared to normal littermates set to 100%. (B) Detailed analysis of kidney weights revealed a permanent reduction in weight for kidneys in all tg animals, but more significant in male mice. At least five animals were used for each time point and data are shown as means ± S.E.M.

Our proEGFcyt tg mouse model suggests a novel in vivo role by which proEGFcyt acts as a negative modulator of the IGF/IGFBP-3 system, specially affecting organs like the kidney and brain known to contain proEGF [35,36]. Since proEGFcyt tg mice lack ossification defects, growth retardation in these mice may be initiated by unknown intracellular processes systemically impacting on the IGF/IGFBP-3 axis. There is a sexual dimorphism for EGF production in the mouse kidney, with higher renal EGF concentrations in females [37,38]. The more pronounced reduction in kidney weight in male as in female proEGFcyt tg mice suggests that higher proEGF concentrations present in female kidneys partially compensate for the renal growth-retarding action of proEGFcyt, an effect ameliorated in male kidneys with lower EGF content. ProEGFcyt can antagonize functions of extracellular EGF in cancer cells [2].

A homozygous mutation with substitution of the conserved proline P1070 by leucine within exon 22 links proEGFcyt to a rare primary hypomagnesemia disorder which is characterized by renal and intestinal magnesium wasting and general symptoms of severe Mg^{2+} depletion [39]. This occurs as a result of impaired basolateral sorting and inadequate renal secretion of EGF into the circulation [39]. ProEGFcyt tg mice contained a functional sorting signal as proEGFcyt displayed basal localization in the tubular epithelial lining of TAL and DC and electrolyte serum levels, including Mg^{2+}, and gene expression of the Mg^{2+} transporters, NCC and NKA, were normal. The distinct cellular localization of human proEGFcyt (basal cellular compartment) and mouse proEGF (luminal membrane) suggests that the human proEGFcyt tg product did not interfere with the normal renal localization/function of endogenous mouse proEGF.

In conclusion, we have identified novel domain-specific in vivo functions of human proEGFcyt with impact on body/organ weight and serum IGFBP-3 levels in mice.

Acknowledgements

The authors thank Dr. H. Steven Wiley, Pacific Northwest National Laboratory, Richland, WA, USA, for providing the human proEGFctF construct. The authors are grateful to C. Froehlich, D. Henderson, P. Perumal, E. Holupirek, and R. Medek for excellent technical support and to Dr. I. Renner-Müller and P. Renner for ani-

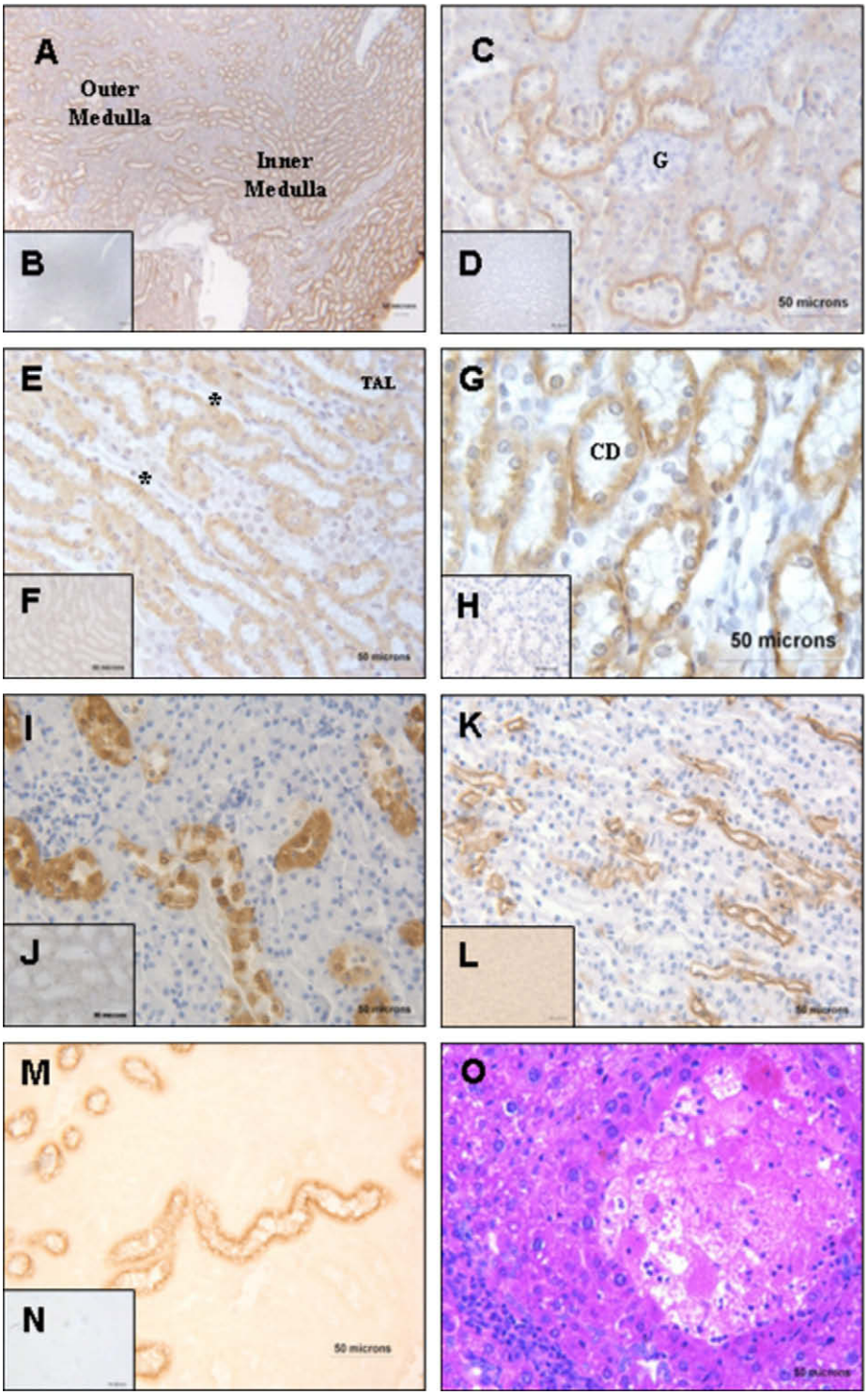

Fig. 6. Immunolocalization of human proEGFcyt in kidney of tg mice (A, C, E, G). ProEGFcyt was present in tubular epithelial cells of the thick ascending loop of Henle (TAL) and of collecting ducts (CD). ProEGFcyt was localized to the basal compartment of tubular epithelial cells (G). The proximal nephron, including the glomerulus (G), proximal tubule, and thin descending loop of Henle (*) were devoid of immunostaining (C, E). Immunoreactive aquaporin-1 (I) and calbindin (K) identified distal tubule/collecting ducts and thin descending loop of Henle, respectively. Mouse EGF was immunodetected in the apical membrane compartment in the same distal nephron parts that expressed human proEGFcyt (M). Hematoxylin–eosin stain of liver tissue revealed isolated necrotic lesions in proEGFcyt mice (O). When the specific antisera were replaced with non-immune serum of the same species no specific immunostaining was observed (B, D, F, H, J, L, N). Magnifications: A, B: ×100; C, D, E, F, N: ×200; I, J, K, L, M, O: ×400; G, H: ×630.

mal management/care. T.K. thanks Dr. J. Wilkins for providing antibodies to AQ-1 and calbindin-D. C.H.-V. and T.K. thank the Deutsche Krebshilfe for generous support. T.K. is grateful to HSCF, MHRC, and NSERC for support. M.R.S. and E.W. thank the German National Genome Research Network for their generous support. M.G. has been supported by a grant from the Deutsche Forschungsgemeinschaft to M.R.S. (GRK1029). A.A.G. was supported by a fellowship from CAPES (Brazil).

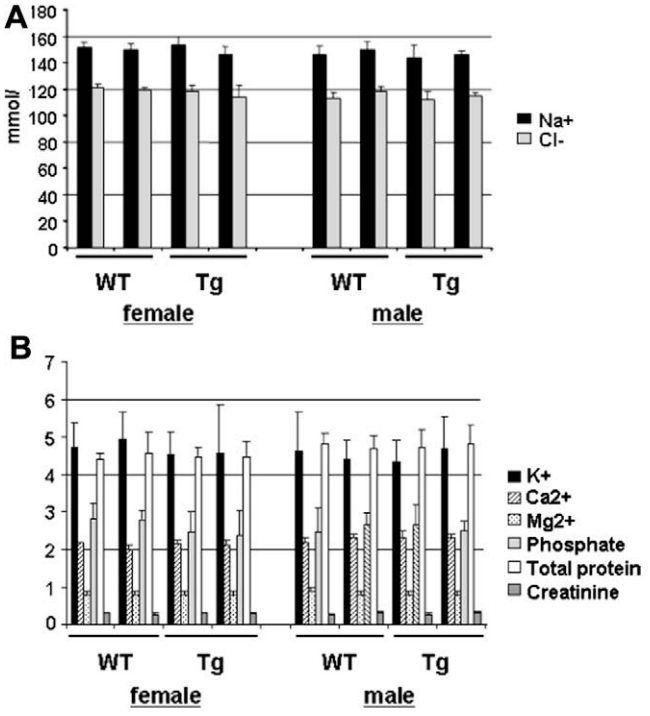

Fig. 7. Measurements of serum levels for (A) Na^+, Cl^- (mmol/l) and (B) K^+, Ca^{2+}, Mg^{2+}, phosphorus (mmol/l), creatinin (mg/dl), and total protein (TP; g/dl) serum levels normal values for proEGFcyt tg mice and normal littermates (five animals at 6 months of age each; data are shown as means ± S.E.M.).

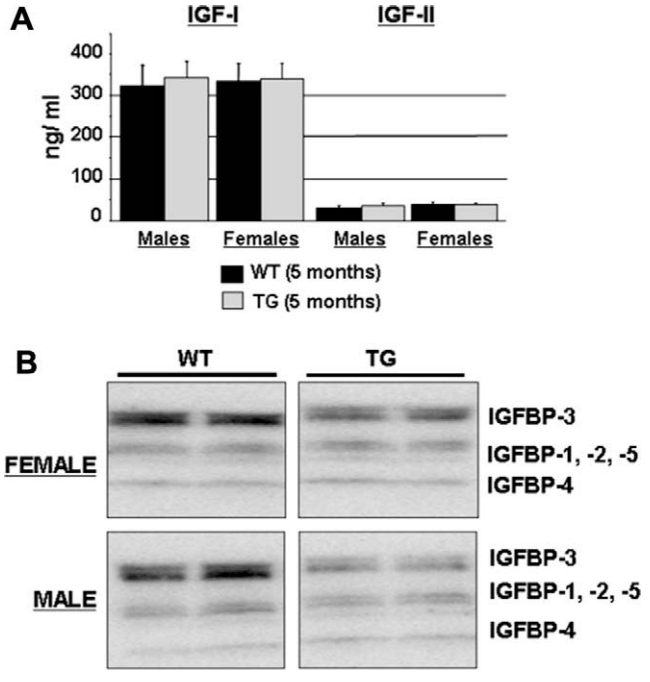

Fig. 8. (A) Radioimmunoassays demonstrated similar serum levels of IGF-I and IGF-II (ng/ml) in five male and female each of tg mice and normal littermates at 5 months of age. (B) Representative Western ligand blot showing serum levels for IGFBP-1 to -5. A total of four tg and wild-type mice were used. Both female and male tg mice displayed exclusive reduction in the level of IGFBP-3 which was most pronounced in male tg mice.

References

[1] Bell, G.I. et al. (1986) Human epidermal growth factor precursor: cDNA sequence, expression in vitro and gene organization. Nucleic Acids Res. 14, 8427–8446.
[2] Glogowska, A. et al. (2008) The cytoplasmic domain of proEGF negatively regulates motility and elastinolytic activity in thyroid carcinoma cells. Neoplasia 10, 1120–1130.
[3] Pyka, J., Glogowska, A., Dralle, H., Hoang-Vu, C. and Klonisch, T. (2005) Cytoplasmic domain of proEGF affects distribution and post-translational modification of microtubuli and increases microtubule-associated proteins 1b and 2 production in human thyroid carcinoma cells. Cancer Res. 65, 1343–1351.
[4] Dempsey, P.J., Meise, K.S. and Coffey, R.J. (2003) Basolateral sorting of transforming growth factor-alpha precursor in polarized epithelial cells: characterization of cytoplasmic domain determinants. Exp. Cell Res. 285, 159–174.
[5] Hieda, M. et al. (2008) Membrane-anchored growth factor, HB-EGF, on the cell surface targeted to the inner nuclear membrane. J. Cell Biol. 180, 763–769.
[6] Nanba, D. and Higashiyama, S. (2004) Dual intracellular signaling by proteolytic cleavage of membrane-anchored heparin-binding EGF-like growth factor. Cytokine Growth Factor Rev. 15, 13–19.
[7] Kinugasa, Y., Hieda, M., Hori, M. and Higashiyama, S. (2007) The carboxyl-terminal fragment of pro-HB-EGF reverses Bcl6-mediated gene repression. J. Biol. Chem. 282, 14797–14806.
[8] Schneider, M.R. and Wolf, E. (2008) The epidermal growth factor receptor ligands at a glance. J. Cell. Physiol. 218, 460–466.
[9] Chan, S.Y. and Wong, R.W. (2000) Expression of epidermal growth factor in transgenic mice causes growth retardation. J. Biol. Chem. 275, 38693–38698.
[10] Wong, R.W., Kwan, R.W., Mak, P.H., Mak, K.K., Sham, M.H. and Chan, S.Y. (2000) Overexpression of epidermal growth factor induced hypospermatogenesis in transgenic mice. J. Biol. Chem. 275, 18297–18301.
[11] Jhappan, C., Stahle, C., Harkins, R.N., Fausto, N., Smith, G.H. and Merlino, G.T. (1990) TGF alpha overexpression in transgenic mice induces liver neoplasia and abnormal development of the mammary gland and pancreas. Cell 61, 1137–1146.
[12] Sandgren, E.P., Luetteke, N.C., Palmiter, R.D., Brinster, R.L. and Lee, D.C. (1990) Overexpression of TGF alpha in transgenic mice. induction of epithelial hyperplasia, pancreatic metaplasia, and carcinoma of the breast. Cell 61, 1121–1135.
[13] Provenzano, A.P., Besner, G.E., James, P.F. and Harding, P.A. (2005) Heparin-binding EGF-like growth factor (HB-EGF) overexpression in transgenic mice downregulates insulin-like growth factor binding protein (IGFBP)-3 and -4 mRNA. Growth Factors 23, 19–31.
[14] Schneider, M.R. et al. (2005) Betacellulin overexpression in transgenic mice causes disproportionate growth, pulmonary hemorrhage syndrome, and complex eye pathology. Endocrinology 146, 5237–5246.
[15] Bachmann, S. et al. (2005) Renal effects of Tamm-Horsfall protein (uromodulin) deficiency in mice. Am. J. Physiol. Renal Physiol. 288, F559–F567.
[16] Blum, W.F. and Breier, B.H. (1994) Radioimmunoassays for IGFs and IGFBPs. Growth Regul. 4 (Suppl. 1), 11–19.
[17] Hossenlopp, P., Seurin, D., Segovia-Quinson, B., Hardouin, S. and Binoux, M. (1986) Analysis of serum insulin-like growth factor binding proteins using western blotting: use of the method for titration of the binding proteins and competitive binding studies. Anal. Biochem. 154, 138–143.
[18] Moerth, C. et al. (2007) Postnatally elevated levels of insulin-like growth factor (IGF)-II fail to rescue the dwarfism of IGF-I-deficient mice except kidney weight. Endocrinology 148, 441–451.
[19] Dong, J., Opresko, L.K., Chrisler, W., Orr, G., Quesenberry, R.D., Lauffenburger, D.A. and Wiley, H.S. (2005) The membrane-anchoring domain of epidermal growth factor receptor ligands dictates their ability to operate in juxtacrine mode. Mol. Biol. Cell 16, 2984–2998.
[20] Dong, J. and Wiley, H.S. (2000) Trafficking and proteolytic release of epidermal growth factor receptor ligands are modulated by their membrane-anchoring domains. J. Biol. Chem. 275, 557–564.
[21] Hida, M., Omori, S. and Awazu, M. (2002) ERK and p38 MAP kinase are required for rat renal development. Kidney Int. 61, 1252–1262.
[22] Hoeflich, A., Schmidt, P., Foll, J., Rottmann, O., Weber, M.M., Kolb, H.J., Pirchner, F. and Wolf, E. (1998) Altered growth of mice divergently selected for body weight is associated with complex changes in the growth hormone/insulin-like growth factor system. Growth Horm. IGF Res. 8, 113–123.
[23] Roelfsema, V. and Clark, R.G. (2001) The growth hormone and insulin-like growth factor axis: its manipulation for the benefit of growth disorders in renal failure. J. Am. Soc. Nephrol. 12, 1297–1306.
[24] Mak, R.H., Cheung, W.W. and Roberts Jr., C.T. (2008) The growth hormone–insulin-like growth factor-I axis in chronic kidney disease. Growth Horm IGF Res. 18, 17–25.
[25] Fernandez-Larrea, J., Merlos-Suarez, A., Urena, J.M., Baselga, J. and Arribas, J. (1999) A role for a PDZ protein in the early secretory pathway for the targeting of proTGF-alpha to the cell surface. Mol. Cell 3, 423–433.
[26] Kuo, A., Zhong, C., Lane, W.S. and Derynck, R. (2000) Transmembrane transforming growth factor-alpha tethers to the PDZ domain-containing, Golgi membrane-associated protein p59/GRASP55. EMBO J. 19, 6427–6439.
[27] Franklin, J.L. et al. (2005) Identification of MAGI-3 as a transforming growth factor-alpha tail binding protein. Exp. Cell Res. 303, 457–470.
[28] Li, C., Franklin, J.L., Graves-Deal, R., Jerome, W.G., Cao, Z. and Coffey, R.J. (2004) Myristoylated Naked2 escorts transforming growth factor alpha to the basolateral plasma membrane of polarized epithelial cells. Proc. Natl. Acad. Sci. USA 101, 5571–5576.

[29] Dempsey, P.J. and Coffey, R.J. (1994) Basolateral targeting and efficient consumption of transforming growth factor-alpha when expressed in Madin-Darby canine kidney cells. J. Biol. Chem. 269, 16878–16889.
[30] Brown, C.L., Coffey, R.J. and Dempsey, P.J. (2001) The proamphiregulin cytoplasmic domain is required for basolateral sorting, but is not essential for constitutive or stimulus-induced processing in polarized Madin-Darby canine kidney cells. J. Biol. Chem. 276, 29538–29549.
[31] Adam, R.M. et al. (2003) A nuclear form of the heparin-binding epidermal growth factor-like growth factor precursor is a feature of aggressive transitional cell carcinoma. Cancer Res. 63, 484–490.
[32] Murphy, L.J., Rajkumar, K. and Molnar, P. (1995) Phenotypic manifestations of insulin-like growth factor binding protein-1 (IGFBP-1) and IGFBP-3 overexpression in transgenic mice. Prog. Growth Factor Res. 6, 425–432.
[33] De Benedetti, F. et al. (2001) Effect of IL-6 on IGF binding protein-3: a study in IL-6 transgenic mice and in patients with systemic juvenile idiopathic arthritis. Endocrinology 142, 4818–4826.
[34] Frystyk, J., Vinter-Jensen, L., Skjaerbaek, C. and Flyvbjerg, A. (1996) The effect of epidermal growth factor on circulating levels of free and total IGF-I and IGF-binding proteins in adult rats. Growth Regul. 6, 48–54.
[35] Fisher, D.A., Salido, E.C. and Barajas, L. (1989) Epidermal growth factor and the kidney. Annu. Rev. Physiol. 51, 67–80.
[36] Lazar, L.M. and Blum, M. (1992) Regional distribution and developmental expression of epidermal growth factor and transforming growth factor-alpha mRNA in mouse brain by a quantitative nuclease protection assay. J. Neurosci. 12, 1688–1697.
[37] Gubits, R.M., Shaw, P.A., Gresik, E.W., Onetti-Muda, A. and Barka, T. (1986) Epidermal growth factor gene expression is regulated differently in mouse kidney and submandibular gland. Endocrinology 119, 1382–1387.
[38] Popliker, M., Shatz, A., Avivi, A., Ullrich, A., Schlessinger, J. and Webb, C.G. (1987) Onset of endogenous synthesis of epidermal growth factor in neonatal mice. Dev. Biol. 119, 38–44.
[39] Groenestege, W.M. et al. (2007) Impaired basolateral sorting of pro-EGF causes isolated recessive renal hypomagnesemia. J. Clin. Invest. 117, 2260–2267.